Earthq Eng & Eng Vib (2011) 10: 37-49 **DOI**: 10.1007/s11803-011-0045-5

Ground motion spatial variability effects on seismic response control of cable-stayed bridges

Shehata E. Abdel Raheem[1†], Toshiro Hayashikawa[2‡] and Uwe Dorka[3‡]

1. *Civil Engineering Department, Faculty of Engineering, Assiut University, Assiut 71516, Egypt*

2. *Bridge and Structural Design Engineering, Hokkaido University, Sapporo, Japan*

3. *Steel & Composite Structures, Kassel Universität, Kassel 34125, Germany*

Abstract: The spatial variability of input ground motion at supporting foundations plays a key role in the structural response of cable-stayed bridges (CSBs); therefore, spatial variation effects should be included in the analysis and design of effective vibration control systems. The control of CSBs represents a challenging and unique problem, with many complexities in modeling, control design and implementation, since the control system should be designed not only to mitigate the dynamic component of the structural response but also to counteract the effects of the pseudo-static component of the response. The spatial variability effects on the feasibility and efficiency of seismic control systems for the vibration control of CSBs are investigated in this paper. The assumption of uniform earthquake motion along the entire bridge may result in quantitative and qualitative differences in seismic response as compared with those produced by uniform motion at all supports. A systematic comparison of passive and active system performance in reducing the structural responses is performed, focusing on the effect of the spatially varying earthquake ground motion on the seismic response of a benchmark CSB model with different control strategies, and demonstrates the importance of accounting for the spatial variability of excitations.

Keywords: cable-stayed bridge; vibration control; earthquake spatial variation; seismic design; semi-active control

1 Introduction

Long span cable-stayed bridges (CSBs) represent aesthetically appealing lifeline structures, and the increasing popularity of these bridges can be attributed to the full and efficient utilization of structural materials, increased stiffness over suspension bridges, efficient and fast mode of construction, and the relatively small size of the substructure (Abdel Raheem and Hayashikawa, 2003; Ali and Abdel-Ghaffar, 1995 a, b). However, from a structural dynamics point of view, long span CSBs exhibit flexible and complex behavior where the vertical, lateral, and torsional motions are often strongly coupled, which raises many concerns about their behavior under environmental dynamic loads such as wind and earthquakes (Fujino, 2002; Ganev *et al*., 1998). The multiple-support problem begins when the bridge is long with regard to the wave-lengths of the input motion in the frequency range of importance to its earthquake response. Then, different parts of the bridge may be subjected to significantly different excitations with a complicated correlation of the motion at the support points. Hence, the spatial variation of the ground displacements and accelerations could play an important role in the determination of the structural response (Lin *et al*., 2004; Lin and Zhang, 2005; Abdel Raheem and Hayashikawa, 2007), as has been shown in recent earthquakes (Loma Prieta 1989, Northridge 1994, Hyogo-Ken Nanbu 1995). Therefore, it is extremely important to include the effects of spatial variation of the ground motion in the analysis, design and tuning of structural systems for the vibration control of seismic induced vibrations of long-span cable-supported bridges. In this way, the control system should be designed not only to mitigate the dynamic component of the structural response, but also to counteract the effects of the pseudo-static component of the response. Harichandran *et al*. (1996) performed a stochastic response analysis of suspension and deck arch bridges to spatially varying earthquake ground motions. They underlined the importance of the effect of spatially varying earthquake ground motions on the response of long span structures. Zerva (1991) evaluated the responses of continuous two- and three-span beams to spatially varying ground motions and examined the validity of the commonly used assumption of equal

Correspondence to: Shehata E. Abdel Raheem, Civil Engineering Department, Faculty of Engineering, Assiut University, Assiut 71516, Egypt
Tel: +20117857478; Fax: +20882332553
E-mail: shehataraheem@yahoo.com
†Associate Professor; ‡Professor

Supported by: Alexander von Humboldt Fellowship-AvH (IV–AGY/1117497 STP) and Japan Society for the Promotion of Science-JSPS Fellowship (P06138)
Received February 8, 2010; **Accepted** November 5, 2010

support motion. Soyluk and Dumanoglu (2004), Soyluk *et al*. (2004) and Lin *et al*. (2004) investigated the effect of spatially varying ground motions including the effect of wave passage, the incoherence of the support motions, and site response. The structures studied were long span cable stayed bridges analyzed in the frequency domain to determine their linear, elastic behavior. Investigation results confirmed that spatial variability and propagation effects of ground motion have important effects on the dynamic behavior of CSBs.

This study investigates the feasibility and efficiency of different control strategies for the seismic protection of CSBs using the benchmark bridge model (Dyke *et al*., 2000). The wave passage effect is more significant than the incoherence effect for the long span bridges subjected to relatively low apparent velocities of wave propagation (Saxena *et al*., 2000). Therefore, the effect of spatial variations of ground motion with different wave propagation apparent velocities on the performance of seismic control systems for CSBs is studied to enhance a structure's ability to withstand dynamic loading. The earthquake excitation of a bridge on multiple supports is derived and the prospects for active and passive control of the bridge motion are explored. Passive systems do not require an external power source and respond to the local motion of the structure. These systems offer the ability to dissipate the vibratory energy in the structure, reducing the number of cycles that the structure will experience (Soong, 1990; Iemura and Pradono, 2002). Semi-active systems generate a control force based on measurements of the structural responses at designated points, hence can adapt to a wide range of operating conditions. The application of semi-active control systems to civil engineering structures is very promising (Abdel Raheem *et al*., 2007; Abdel Raheem and Dorka, 2006; Caicedo *et al*., 2003; Jansen and Dyke, 2002). Control forces are developed based on feedback from sensors that measure the excitation and/or the response of the structure, and the feedback of the response may be measured at locations remote from the active control systems. With hysteretic device systems, *HYDES* (Dorka *et al*., 1998) being independent of the vertical load bearing system, a wide variety of link hysteresis loops are possible for optimal performance, and complete control over the maximum forces is possible in the main horizontal load resisting system regardless of the type and severity of the earthquake. To effectively implement control systems on structural systems, it is necessary to know which type of control system will achieve better performance on the structure under consideration. This will lead to the development of guidelines for selecting the most appropriate control system for a structure. A systematic comparison of passive and active systems performance in reducing the structure responses is performed in this study.

The effects of spatially varying earthquake ground motions on the controlled long span bridges are not comprehensively investigated. For this reason, the focus of this study is to investigate the effect of the spatially varying earthquake ground motion on the seismic response of CSB with different control strategies. The effect of the spatial variability of the ground motion in the analysis of seismically controlled long span bridges is considered based on the decomposition of the total structural response into a dynamic component and a pseudo-static component. Comparison of the controlled CSB response due to non-uniform input of different wave propagation velocities with the response due to uniform input demonstrates the importance of accounting for spatial variability of excitations. The control systems are shown to perform well when earthquake motions are uniform at all supports along the entire CSB, however, under multiple-support excitations, the performance of the control system with these parameters becomes worse dramatically over almost all of the evaluation criteria. Moreover, bridges subjected to spatially variable input motions are characterized by excitation of higher modes which are primarily anti-symmetric. The assumption of uniform earthquake motion along the entire bridge, however, may be unrealistic for long span bridges since the differences in ground motion among different supports due to traveling seismic waves may result in quantitative and qualitative differences in seismic response as compared with those produced by uniform motion at all supports. Design codes and retrofitting techniques must be upgraded to take into account the spatial character of the seismic input.

2 Finite element model formulation

Based on detailed drawings of the CSB shown in Fig. 1, a three-dimensional finite element model has been developed (Dyke *et al*., 2000; Caicedo *et al*., 2003) to represent the complex behaviour of the full-scale benchmark bridge shown in Fig 2. The finite element model employs beam elements, cable elements and rigid links. Constraints are applied to restrict the deck from moving in the lateral direction at Piers 2, 3 and 4. Boundary conditions restrict the motion at Bent 1 to allow only longitudinal displacement (X) and rotations about the Y and Z axes. Because the attachment points of the cables to the deck are above the neutral axis of the deck, and the attachment points of the cables to the tower are outside the neutral axis of the tower, rigid links are used to connect the cables to the tower and to the deck. The use of the rigid links ensures that the length and inclination angle of the cables in the model agree with the drawings. Additionally, the moment induced in the towers by the movement of the cables is taken into consideration. The cables are modelled with truss elements; the nominal tension is assigned to each cable. Nonlinear static analysis is performed in ABAQUS®, and the element mass and stiffness matrices are output to MATLAB® for assembly. Subsequently, the constraints are applied, and a reduction is performed to reduce the model to a more manageable size.

A modified evaluation model is formed in which

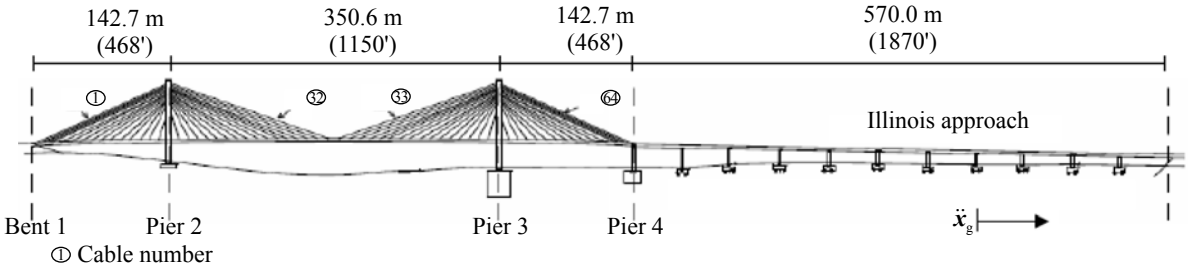

Fig. 1 View of the Cape Girardeau Bridge

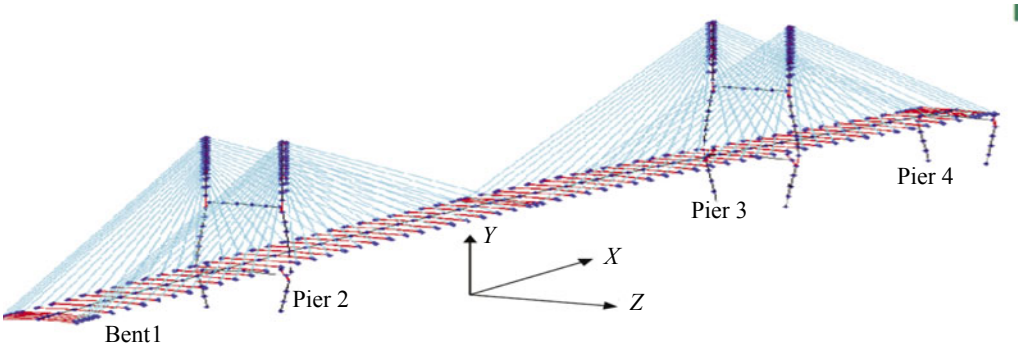

Fig. 2 Bridge finite element model

the connections between the tower and the deck are disconnected. The first ten undamped frequencies of the model are 0.2899, 0.3699, 0.4683, 0.5158, 0.5812, 0.6490, 0.6687, 0.6970, 0.7102, and 0.7203 Hz. The uncontrolled structure used as a basis of comparison for the controlled system corresponds to the former model in which the deck-tower connections are fixed (the dynamically stiff shock transmission devices are present). Additionally, the deck is constrained in the vertical direction at the towers. The bearings at Bent 1 and Pier 4 are designed to permit longitudinal displacement and rotation about the transverse and vertical axis.

An important feature of CSBs is the effect of the dead load that may contribute to 80%–90% of the total bridge loads. Dead loads are usually applied before the earthquake, so that the seismic analysis should start from the deformed equilibrium configuration due to dead loads. The linear evaluation model that was developed and used as a basis of comparison of the performance using various protective systems is considered in this study. Three earthquake records, each scaled to a peak ground acceleration (PGA) of 0.36 g or smaller, that are used for numerical simulations are: (i) El Centro NS (1940); (ii) Mexico City (1985); and (iii) Gebze N-S (1999). Evaluation criteria J_1 to J_{18} have been established (Dyke *et al*., 2000; Caicedo *et al*., 2003); however, only the evaluation criteria J_1 to J_{13} are relevant to semi-active and passive systems and hence used in the present study. These evaluation criteria have been normalized by the corresponding response quantities for the uncontrolled bridge. Considering the general equation of motion for a CSB subjected to uniform seismic loads, the dynamic equation of motion can be written as

$$\boldsymbol{M}\ddot{\boldsymbol{U}} + \boldsymbol{C}\dot{\boldsymbol{U}} + \boldsymbol{K}\boldsymbol{U} = -\boldsymbol{M}\boldsymbol{\Gamma}\ddot{x}_g + \boldsymbol{\Lambda}\boldsymbol{f} \tag{1}$$

where $\boldsymbol{U}$ is the displacement response vector, $\boldsymbol{M}$, $\boldsymbol{C}$ and $\boldsymbol{K}$ are the mass, damping and stiffness matrices of the structure, $\boldsymbol{f}$ is the vector of control force inputs, $\ddot{x}_g$ is the longitudinal ground acceleration, $\boldsymbol{\Gamma}$ is a vector of zeros and ones relating the ground acceleration to the bridge degrees of freedom (DOF), and $\boldsymbol{\Lambda}$ is a vector relating the force produced by the control device to the bridge DOFs. This is appropriate when the excitation is uniformly applied at all the structural supports. For the analysis with multiple-support excitation, the bridge model must include the supports for the degrees of freedom. The equation of dynamic equilibrium for all the DOFs is written in partitioned form (Caicedo *et al*., 2003).

$$\begin{bmatrix} \boldsymbol{M} & \boldsymbol{M}_g \\ \boldsymbol{M}_g^{\mathrm{T}} & \boldsymbol{M}_{gg} \end{bmatrix} \begin{bmatrix} \ddot{\boldsymbol{U}}_t \\ \ddot{\boldsymbol{U}}_g \end{bmatrix} + \begin{bmatrix} \boldsymbol{C} & \boldsymbol{C}_g \\ \boldsymbol{C}_g^{\mathrm{T}} & \boldsymbol{C}_{gg} \end{bmatrix} \begin{bmatrix} \dot{\boldsymbol{U}}_t \\ \dot{\boldsymbol{U}}_g \end{bmatrix} + \begin{bmatrix} \boldsymbol{K} & \boldsymbol{K}_g \\ \boldsymbol{K}_g^{\mathrm{T}} & \boldsymbol{K}_{gg} \end{bmatrix} \begin{bmatrix} \boldsymbol{U}_t \\ \boldsymbol{U}_g \end{bmatrix} = \begin{bmatrix} \boldsymbol{O} \\ \boldsymbol{P}_g \end{bmatrix} + \begin{bmatrix} \boldsymbol{\Lambda}\boldsymbol{f} \\ \boldsymbol{O} \end{bmatrix} \tag{2}$$

where $\boldsymbol{U}_t$ and $\boldsymbol{U}_g$ are the superstructure absolute displacement vector and the supports enforced ground displacement vector, respectively; $\boldsymbol{M}_g$, $\boldsymbol{C}_g$ and $\boldsymbol{K}_g$ are the mass, damping and elastic-coupling matrices expressing the forces developed in the active DOFs by the motion of the supports. $\boldsymbol{M}_{gg}$, $\boldsymbol{C}_{gg}$ and $\boldsymbol{K}_{gg}$ are the mass, damping and stiffness matrices of the supports, respectively. It is desired to determine the displacement vector $\boldsymbol{U}_t$ in the superstructure DOFs and the support forces $\boldsymbol{P}_g$,

since the control forces $\boldsymbol{f}$ are only applied to the active superstructure DOFs. The total displacement $\boldsymbol{U}_t$ is expressed as its displacement $\boldsymbol{U}_s$ due to static application of the ground motion, plus the dynamic displacement $\boldsymbol{U}$ relative to the quasi-static displacement.

$$\boldsymbol{U}_t = \boldsymbol{U}_s + \boldsymbol{U} \tag{3}$$

$$\boldsymbol{K}\boldsymbol{U}_s + \boldsymbol{K}_g\boldsymbol{U}_g = \boldsymbol{0} \tag{4}$$

In which, $\boldsymbol{U}_s$ is the pseudo-static displacement vector. In the model, the seismic movement of the bridge supports excites the superstructure of the bridge through the influence matrix. Solving for these displacements leads to the pseudo-static influence vector to be defined as follows

$$\boldsymbol{R}_s = -\boldsymbol{K}^{-1}\boldsymbol{K}_g \tag{5}$$

Finally, substituting Eqs. (3), (4) and Eq. (5) into the first row of Eq. (2) gives

$$\boldsymbol{M}\ddot{\boldsymbol{U}} + \boldsymbol{C}\dot{\boldsymbol{U}} + \boldsymbol{K}\boldsymbol{U} = \boldsymbol{\Lambda}\boldsymbol{f} - (\boldsymbol{M}\boldsymbol{R}_s + \boldsymbol{M}_g)\,\ddot{\boldsymbol{U}}_g - (\boldsymbol{C}\boldsymbol{R}_s + \boldsymbol{C}_g)\dot{\boldsymbol{U}}_g \tag{6}$$

If the ground accelerations $\ddot{\boldsymbol{U}}_g$ and velocities $\dot{\boldsymbol{U}}_g$ are prescribed at each bridge support, this completes the governing equation formulation. The excitations are in fact non-uniform for different foundations. In this analysis, the non-uniformity of the ground accelerations is realized by using the same seismic waves but with time delays.

The model resulting from the finite element formulation, which is modelled by beam elements, cable elements, and rigid links as shown in Fig. 2, has a large number of DOFs and high frequency dynamics. Thus, some assumptions are made to make the model more manageable for dynamic simulation while retaining the fundamental behavior of the bridge. Application of the static condensation reduction scheme to the full model of the bridge resulted in a reduced order model of 419 DOFs, its first 100 natural frequencies (up to 3.5 Hz) were compared and are in good agreement with those of the 909 DOF structure. The damping matrix is defined based on a modal damping assumption and developed by assigning 3% of critical damping to each mode, and this value is selected to be consistent with assumptions made during the bridge design. The evaluation model is considered to portray the actual dynamics of the bridge and will be used to evaluate various control systems. Because the evaluation model is too large for control design and implementation, a reduced-order model (i.e., design model) of the system should be developed. The design model (Dyke *et al*., 2000; Caicedo *et al*., 2003) has 30 states, and was derived from the evaluation model by forming a balanced realization of the system and condensing out the states with relatively small controllability and observability Grammians.

3 Analytical model and control strategy

For a seismically excited structure, assuming that the forces provided by the control devices are adequate to keep the seismic response of the structure within the linear region, the equations of motion can be written in the state-space form description as follows:

$$\dot{\boldsymbol{x}} = \boldsymbol{A}\boldsymbol{x} + \boldsymbol{B}\boldsymbol{f} + \boldsymbol{E}\left[\ddot{\boldsymbol{U}}_g^{\mathrm{T}}\ \dot{\boldsymbol{U}}_g^{\mathrm{T}}\right]^{\mathrm{T}} \tag{7}$$

$$\boldsymbol{y}_m = \boldsymbol{C}_y\boldsymbol{x} + \boldsymbol{D}_y\boldsymbol{f} + \boldsymbol{v} \tag{8}$$

$$\boldsymbol{z} = \boldsymbol{C}_z\boldsymbol{x} + \boldsymbol{D}_z\boldsymbol{f} \tag{9}$$

In which $\boldsymbol{x}$ is the state vector, $\boldsymbol{y}_m$ is the vector of measured outputs, $\boldsymbol{z}$ is the regulated output vector and $\boldsymbol{v}$ is the measurement noise vector. The measurements typically available for control force determination include the absolute acceleration of selected points on the structure, the displacement of each control device, and a measurement of each control force. For this initial study, the active, semi-active and passive devices are modeled as ideal devices. Therefore, neither actuator dynamic nor control-structure interaction is explicitly included in the device models. The approach used for the model and control devices is described in the following sections.

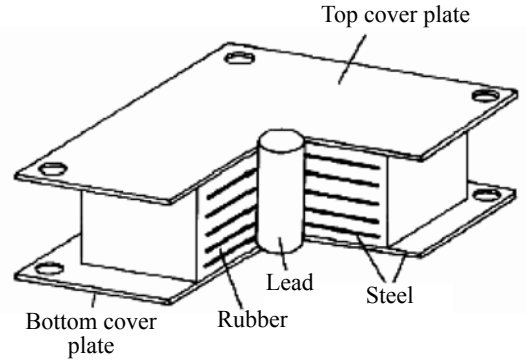

(a) LRB construction scheme

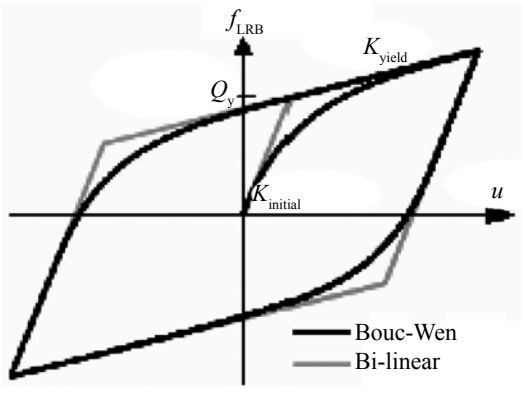

(b) Hysteretic model

Fig. 3 Passive control device

3.1 Passive control system

One of the most widely implemented and accepted seismic protection systems is base isolation. The seismic isolation, with a lengthened natural period to limit displacement, which is known as "the Menshin Design," has been widely accepted in highway bridges in Japan following the 1995 Hyogo-ken Nanbu earthquake. A passive control system based on elastomeric lead-rubber bearings (LRBs) has been adopted as a retrofit strategy, because it limits the transfer of the input seismic energy to the structure. Hence, most of the displacements occur across the device, while the superstructure deforms pretty much as a rigid body. The design shear force level for the yielding of lead plugs that equal to 0.10 of the deck weight carried by bearings has been widely accepted among bearing designers (Ali and Abdel-Ghaffar, 1995 a, b; Robinson, 1982). The passive control forces applied to the structure are only dependent on the motion of the structure and are a function of the relative displacement and velocity across the device. The compliant LRBs installed in the bridge deck tower/bent connection of a seismically isolated bridge structure protect it from strong earthquakes. In this study, LRBs are used as damping energy dissipation devices, which simply generate longitudinal restoring force. A parametric analysis has been performed to obtain the optimal values of the yielding forces and the post-yield stiffness by considering them as objective functions of the moments of the piers and the displacement of the deck. The adopted parameters have been considered in order to optimize the response reduction. Isolation bearings were designed to accommodate large displacement demands and to mobilize damping mechanisms, typically through material yielding of a lead column within the isolator as shown in Fig. 3. A nonlinear yielding hysteretic dissipative Bouc-Wen model is adopted to represent the dynamic behavior of LRB isolators under severe earthquakes.

3.2 Semi-active control system

The H2/LQG control algorithm is used for the controller design using the reduced order model of the system (Dyke *et al*., 1996; Abdel Raheem *et al*., 2008). Optimal control algorithms are based on the minimization of a performance index that depends on the system variables, while maintaining a desired system state and minimizing the control effort. The active control force $\boldsymbol{f}_c$ is found by minimizing the performance index subjected to a second order system. A nonlinear control law is derived to maximize the energy dissipated from a vibrating structure by the frictional interface using the normal force as the control input. The level of normal force required is determined using an optimal controller; the LQG control problem is to devise a control law with constant gain to minimize the quadratic cost function in the form

$$\boldsymbol{f}_c = -\boldsymbol{K}_c\, \boldsymbol{x} \tag{10}$$

In the design of the controller, the disturbances to the system are taken to be an identically distributed, statistically independent stationary white noise process. An infinite horizon performance index is chosen that weights the regulated output vector, $\boldsymbol{z}$

$$J = \lim_{\tau\to\infty}\frac{1}{\tau}\mathrm{E}\left[\int_0^{\tau}\left\{(\boldsymbol{C}_z\boldsymbol{x}+\boldsymbol{D}_z\boldsymbol{f})^{\mathrm{T}}\boldsymbol{Q}(\boldsymbol{C}_z\boldsymbol{x}+\boldsymbol{D}_z\boldsymbol{f})+\boldsymbol{f}^{\mathrm{T}}\boldsymbol{R}\boldsymbol{f}\right\}\mathrm{d}t\right] \tag{11}$$

where $\boldsymbol{Q}$ and $\boldsymbol{R}$ are weighting matrices for the vectors of regulated responses and control forces, respectively. Furthermore, the measurement noise is assumed to be identically distributed, statistically independent Gaussian white noise process, with $S_w / S_v = \gamma = 25$, where S_w and S_v are the autospectral density function of ground acceleration and measurement noise. $\boldsymbol{K}_c$ is the full state feedback gain matrix for the deterministic regulator problem. The problem with state feedback control is that every element of the state vector is used in the feedback path and, clearly, many states in realistic systems are not easily measurable. The optimal controller Eq. (10) is not implemented without the full state measurement. However, a state estimate can be formulated $\hat{\boldsymbol{x}}$ such that $\boldsymbol{f}_c = -\boldsymbol{K}_c\hat{\boldsymbol{x}}$ remains optimal based on the measurements. This state estimate is generated by the Kalman filter

$$\dot{\hat{\boldsymbol{x}}} = \boldsymbol{A}\hat{\boldsymbol{x}} + \boldsymbol{B}\boldsymbol{f}_m + \boldsymbol{L}(\boldsymbol{y}_m - \boldsymbol{C}_y\hat{\boldsymbol{x}} - \boldsymbol{D}_y\boldsymbol{f}_m) \quad = (\boldsymbol{A}-\boldsymbol{L}\boldsymbol{C}_y)\hat{\boldsymbol{x}} + \left[\boldsymbol{L}\ \ \boldsymbol{B}-\boldsymbol{L}\boldsymbol{D}_y\right]\begin{Bmatrix}\boldsymbol{y}_m\\ \boldsymbol{f}_m\end{Bmatrix} \tag{12}$$

In which $\hat{\boldsymbol{x}}$ is the Kalman filter optimal estimate of the state space vector $\boldsymbol{x}$. $\boldsymbol{L}$ is the gain matrix for state estimator with the state observer technique, which is determined by solving an algebraic Riccati equation where the estimator uses the known inputs $\boldsymbol{f}_c$ and the measurements $\boldsymbol{y}_m$ to generate the output and state estimates $\hat{\boldsymbol{y}}$ and $\hat{\boldsymbol{x}}$. A Kalman filter was used to estimate the states of the reduced-order model required for the applications of semi-active controllers using selected acceleration and displacement measurements. The proposed approach is to append a force feedback loop to induce the friction device to produce an approximately desired control force $\boldsymbol{f}_c$. A linear optimal controller $\boldsymbol{K}_c(s)$ is then designed that provides the desired control force $\boldsymbol{f}_c$ based on the measured responses $\boldsymbol{y}_m$, and the measured force $\boldsymbol{f}_m$ as follows

$$\boldsymbol{f}_c = L^{-1}\left\{-\boldsymbol{K}_c(s)L\left(\begin{bmatrix}\boldsymbol{y}_m\\ \boldsymbol{f}_m\end{bmatrix}\right)\right\} \tag{13}$$

where L (.) is the Laplace transform. Although the controller $\boldsymbol{K}_c(s)$ can be obtained from a variety of synthesis methods, the H2/LQG strategies are advocated herein because of the stochastic nature of earthquake

ground motions and because of their successful application in other civil engineering structural control applications. The force generated by the friction device cannot be commanded; only the voltage v applied to the current driver for the friction device can be directly changed, and consequently, the air pressure could be changed. To induce the friction device to generate approximately the device desired optimal control force f_{ci}, the algorithm for selecting the command signal v_i for the ith device can be concisely stated as follows

$$v_i = (V_{\max} / f_{\max}) \mid f_{ci} \mid H(\{f_{ci} - f_{mi}\} f_{mi}) \tag{14}$$

where $V_{\max}$ and $f_{\max}$ is the device maximum voltage and force, and $H(.)$ is the Heaviside step function.

The friction device UHYDE-fbr dissipates energy as a result of solid sliding friction (Abdel Raheem and Dorka, 2006; Dorka *et al*., 1998). The patented sliding mechanism consists of two steel plates and a set of bronze inserts. One of the steel plates serves as guidance for the bronze inserts. The other plate has a specially prepared surface which is in contact with the inserts forming the sliding surface as shown in Fig.4. The structural implementation of these devices as well as the experimental verification and evaluation of semi-active control in bridges has been experimentally investigated at the European Laboratory for Structural Assessment within the "Testing of Algorithms for Semi-Active Control of Bridges (TASCB)" project, financed under the "European Consortium of Laboratories for Earthquake And Dynamic Experimental Research - JRC" (ECOLEADER) within the Fifth Framework Program of the European Commission.

In a well designed control system, the earthquake input energy is largely dissipated in the control devices through friction or yielding of a lead plug. The devices limit the motion of the mechanism which leads to minimized stresses in the structure. The Bouc–Wen's model is used to characterize the hysteretic force-deformation of the UHYDE-fbr and LRB devices. The forces mobilized in the control device can be modeled by a biaxial model as follows:

$$\begin{aligned} f_x &= c_0 \dot{u}_x + k_0 u_x + \alpha z_x \\ f_y &= c_0 \dot{u}_y + k_0 u_y + \alpha z_y \end{aligned} \tag{15}$$

where z_i is an evolutionary shape variable, internal friction state, bounded by the values ± 1; and account for the conditions of separation and reattachment (instead of a signum function) and the directional/biaxial interaction of device forces. The determination of the most appropriate yielding level or slip load level at different placement locations in the structure is, thus, an important design issue which must be resolved for effective utilization of the devices in practice.

From displacement controlled tests on the friction device under constant pressure and varying frequency, no significant dependency of the friction coefficient on the excitation frequency was observed and the average friction coefficient is determined to be 0.45. In this paper, the dynamic behavior is neglected, so the normal force is proportional to the input voltage. In addition, the dynamics involved in the UHYDE-fbr pneumatic servo system equilibrium are accounted for through the first order filter

$$\dot{u} = -\eta(u - v) \tag{16}$$

where v is the command voltage applied to the control circuit, and η = 50 s^{-1} is a time constant associated with a filter. Analog voltage control, cover range 0 – 10 Volt, is applied to the air pressure regulator to set the desired analog output air pressure signal. The functional dependence of the device parameters on the command voltage u is expressed as:

$$\alpha = \alpha_a + \alpha_b u \;;\; c_0 = c_{0a} + c_{0b} u \tag{17}$$

In Eqs. (15) & (17), $\alpha = \mu N$ is function of N being the clamping force and μ the coefficient of sliding friction, and c_0 describes the force associated with viscous dissipation due to compressed gas. The parameters of the UHYDE-fbr device are selected so that the device has a capacity of 1000 kN and maximum displacement of 500 mm (the tested friction device scaled: 2.5 for the

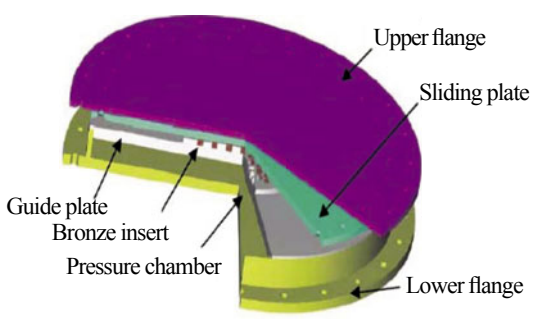

(a) UHYDE-fbr developed by Dorka

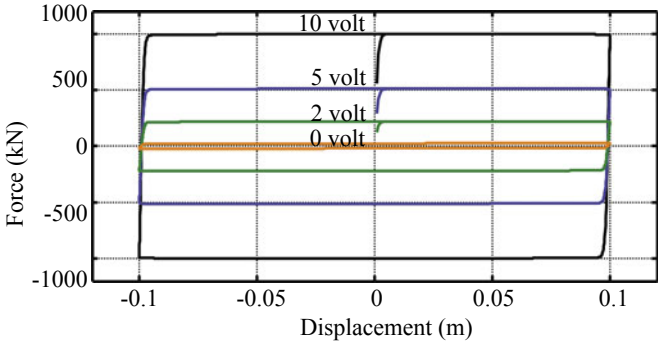

(b) Hysteretic model for different input volt

Fig. 4 Semi-active control device

frictional force; 1.5 for displacement), as follows: A = 1000 m^{-1} and $\gamma = \beta$ = 500 m^{-1}, c_{0a} = 10 kN·s/m, c_{0b} = 25 kN·s/(m·V), k_0 = 25 kN/m, α_a = 22.5 kN, α_b = 101.25 kN/V. The horizontal nonlinear restoring force is expressed as the sum of three forces acting in parallel given in Eq. (15), in which for passive control, k_0 and c_0 are the horizontal stiffness and viscous damping coefficient of the rubber composite of the bearing. α = (1- k_0/k_e) .Q_y is the yield force of the lead plug; Q_y is the yield force from both the lead plug and the rubber stiffness. The properties of the LRB are k_e initial elastic shear stiffness and k_0 post-yield shear stiffness, k_0/k_e = 0.10. To model the initial stiffness properly, it is required that $A = k_e/Q_y$. For unloading to follow the pre-yield stiffness, A = 140 m^{-1} and $\gamma = \beta$ = 70 m^{-1}, c_0 = 100 kN·s/m, k_e = 68000 kN/m, and Q_y = 400 kN.

4 Numerical results and discussions

To verify the effectiveness of the presented seismic control design, simulations are performed for the three historical earthquakes specified in the benchmark problem statement. The spatially varying earthquake wave propagation is assumed in the subsoil from one end of the bridge to the other. Three propagating velocities of the seismic wave in the soil 1000 and 3000m/s, as well as with infinite speed (uniform excitation) are used in the simulations. To evaluate the capability of various control systems for reducing the peak responses, the normalized responses over the entire time record, and the control requirements, eighteen criteria have been defined (Dyke *et al*., 2000; Caicedo *et al*., 2003) to evaluate the capabilities of each proposed control strategy. Thirteen evaluation criteria J_1–J_{13} are considered in this study, the first six consider the ability of the controller to reduce peak responses; evaluation criteria J_1–J_6 are related to peak response quantities, where J_1 = the peak base shear of towers, J_2 = the peak shear force of towers at the deck level, J_3 = the peak overturning moment at the bases of towers, J_4 = the peak moment of towers at the deck level, J_5 = the peak deviation in cable tension, and J_6 = the peak displacement of the deck at the abutment.

$$J_1 = \max_{\substack{ElCentro\\Mexico\\Gebze}} \left\{ \frac{\max_{i,t} |F_{bi}(t)|}{F_{0b}^{\max}} \right\}, \quad J_2 = \max_{\substack{ElCentro\\Mexico\\Gebze}} \left\{ \frac{\max_{i,t} |F_{di}(t)|}{F_{0d}^{\max}} \right\}$$

$$J_3 = \max_{\substack{ElCentro\\Mexico\\Gebze}} \left\{ \frac{\max_{i,t} |M_{bi}(t)|}{M_{0b}^{\max}} \right\}, \quad J_4 = \max_{\substack{ElCentro\\Mexico\\Gebze}} \left\{ \frac{\max_{i,t} |M_{di}(t)|}{M_{0d}^{\max}} \right\}$$

$$J_5 = \max_{\substack{ElCentro\\Mexico\\Gebze}} \left\{ \max_{i,t} \left| \frac{T_{ai} - T_{0i}}{T_{0i}} \right| \right\}, \quad J_6 = \max_{\substack{ElCentro\\Mexico\\Gebze}} \left\{ \max_{i,t} \left| \frac{x_{bi}(t)}{x_{0i}} \right| \right\}$$

where $F_{bi}(t)$ and $F_{di}(t)$, $M_{bi}(t)$ and $M_{di}(t)$ are the base shear and moment, shear and moment at the deck level in the i-th tower, $F_{0b}^{\max}$ and $M_{0b}^{\max}$, $F_{0d}^{\max}$ and $M_{0d}^{\max}$ are the maximum uncontrolled base shear and moment, shear and moment at the deck level in the two towers. T_{0i} is the nominal pretension in the ith cable, $T_{ai}(t)$ is the actual tension in the cable, and x_{0b} is the maximum of the uncontrolled deck response at these locations. Evaluation criteria J_7–J_{11} are related to normed response quantities corresponding to response quantities for J_1–J_5.

$$J_7 = \max_{\substack{ElCentro\\Mexico\\Gebze}} \left\{ \frac{\max_{i} \|F_{bi}(t)\|}{\|F_{0b}\|} \right\}, \quad J_8 = \max_{\substack{ElCentro\\Mexico\\Gebze}} \left\{ \frac{\max_{i} \|F_{di}(t)\|}{\|F_{0d}\|} \right\}$$

$$J_9 = \max_{\substack{ElCentro\\Mexico\\Gebze}} \left\{ \frac{\max_{i} \|M_{bi}(t)\|}{\|M_{0b}\|} \right\}, \quad J_{10} = \max_{\substack{ElCentro\\Mexico\\Gebze}} \left\{ \frac{\max_{i} \|M_{di}(t)\|}{\|M_{0d}\|} \right\}$$

$$J_{11} = \max_{\substack{ElCentro\\Mexico\\Gebze}} \left\{ \max_{i} \frac{\|T_{ai} - T_{0i}\|}{T_{0i}} \right\}, \qquad \|.\| \equiv \sqrt{\frac{1}{t_f} \int_0^{t_f} (.)^2 \, \mathrm{d}t}$$

Evaluation criteria J_{12} –J_{13} are related to control system requirements; J_{12} = the peak control force, J_{13} = the peak device stroke.

$$J_{12} = \max_{\substack{ElCentro\\Mexico\\Gebze}} \left\{ \max_{i,t} \left(\frac{f_i(t)}{W} \right) \right\}, \quad J_{13} = \max_{\substack{ElCentro\\Mexico\\Gebze}} \left\{ \max_{i,t} \left(\frac{|y_i^{\mathrm{d}}(t)|}{x_0^{\max}} \right) \right\}$$

where $f_i(t)$ is the force generated by the i-th control device over the time history, W = 510×10^3 kN is the seismic weight of a bridge based on the mass of the superstructure, $y_i^{\mathrm{d}}(t)$ is the stroke of the i-th control device, and $x_0^{\max}$ is the maximum uncontrolled displacement at the top of the towers relative to the ground.

In the *Passive Control Strategy*, 24 LRBs are placed between the deck and pier/bent at eight locations in the bridge, eight between the deck and Pier 2, eight between the Deck and Pier 3, four between the Deck and Bent 1, and four between the Deck and Pier 4. The device parameters are optimized for maximum energy dissipation and to minimize the earthquake force and displacement responses.

In the *Active Control Strategy*, ideal hydraulic actuators are used and an H2/LQG control algorithm is adopted. 24 actuators are used for sample active control described in the benchmark, while 24 friction devices are used for semi-active control on the bridge with a configuration as in the passive strategy. In addition to fourteen accelerometers, eight displacement transducers and eight force transducers to measure control forces applied to the structure are used for feedback to the clipped optimal control algorithm. To evaluate the ability of the friction device system

in achieving the performance of a comparable fully active control system, the device is assumed to be ideal, and can generate the desired dissipative forces with no delay, hence the actuator/sensor dynamics are not considered. Appropriate selection of parameters ($\boldsymbol{z}$, $\boldsymbol{Q}$, $\boldsymbol{R}$) is important in the design of the control algorithm to achieve high performance controllers. The weighting coefficients of the performance index were selected such that $\boldsymbol{R}$ was selected as an identity matrix; and $\boldsymbol{z}$ is comprised of different important responses for the overall behavior of the bridge that are constructed by the Kalman filter from selected measurements. Extensive simulations have been conducted to find the most effective weighting values corresponding to regulated responses, and accordingly, the optimized weighting matrix $\boldsymbol{Q}$ can be selected as follows:

For Semi-active control with feedback corresponding to deck displacement and mid span velocity regulated output response and weighting values as:

$$\boldsymbol{Q}_{\mathrm{d}d\,\&\,\mathrm{d}v}=\begin{bmatrix} q_{\mathrm{d}d}\boldsymbol{I}_{4\mathrm{x}4} & 0 \\ 0 & q_{\mathrm{d}v} \end{bmatrix} \quad q_{\mathrm{d}d}=8092.5,\ q_{\mathrm{d}v}=4.607\times10^{5}$$

For Sample active control with feedback corresponding to the deck displacement and mid span acceleration regulated output response and weighting values as:

$$\boldsymbol{Q}_{\mathrm{d}d\,\&\,\mathrm{d}a}=\begin{bmatrix} q_{\mathrm{d}d}\boldsymbol{I}_{4\mathrm{x}4} & 0 \\ 0 & q_{\mathrm{d}a} \end{bmatrix} \quad q_{\mathrm{d}d}=3222\ ,\ q_{\mathrm{d}a}=40.0$$

Simulation results of the proposed control strategies are compared for the uniform and the multiple excitation with two shear wave velocities of 3000 and 1000 m/s. Tables 1–3 show the evaluation criteria for all three earthquakes. Note that the different control strategies are very effective in reducing the force and displacement response, especially for ground motions with a high frequency content such as El Centro with dominant frequencies of 1.1, 1.3 and 2.1 Hz, as shown in Table 1, while the efficiency of control strategies under the Mexico earthquake (dominant frequency of 0.45 Hz) and Gebze earthquake (dominant frequencies of 0.25 and 2.0 Hz) that have a lower frequency content, is decreased and results in larger force and displacement responses dominated by low-order modes compared to the El Centro earthquake case shown in Tables 1–3. It is also shown that the dependency of the seismic response of the controlled bridge on the frequency content of the input motion, since lower and higher order fundamental modes with frequencies close to Gebze earthquake wide range dominant frequencies are excited, results in higher force and displacement responses, and thus a higher control force is required. It is observed that the different control strategies are quite effective in reducing response quantities of the bridge whenever the predominant period of ground motions is close to the fundamental natural period of the bridge and less effective when the former is far from the latter. The maximum deck displacement is less than allowable displacement (0.3 m), and the tension in the stay cables remains within allowable values.

A comparative study was also performed on a CSB benchmark equipped with passive, semi-active and active control systems with the same number and configuration of control devices. The passive control strategy can be designed to achieve a peak response (J_1 –J_6) reduction comparable to the active/semi-active control strategy. However, since it is difficult to attain the same response reduction efficiency over the entire time history (J_7 –J_{11}), the member force responses can be minimized, but of

Table 1 Maximum evaluation criteria for El Centro earthquake

Criteria	Passive control			Semi-active control			Sample active control		
	Uniform	Multiple excitation, v_s		Uniform	Multiple excitation, v_s		Uniform	Multiple excitation, v_s	
	∞ m/s	3000 m/s	1000 m/s	∞ m/s	3000 m/s	1000 m/s	∞ m/s	3000 m/s	1000 m/s
J_1	0.2816	0.2867	0.3346	0.2908	0.3229	0.2921	0.2711	0.3048	0.3236
J_2	0.8258	1.0108	1.1745	0.9058	0.8532	0.9307	0.7645	0.7911	1.1366
J_3	0.3144	0.3621	0.3749	0.2339	0.2940	0.2345	0.2816	0.3458	0.3423
J_4	0.6998	0.6468	0.5642	0.4805	0.4988	0.4872	0.5744	0.5572	0.5704
J_5	0.2826	0.2235	0.3197	0.2732	0.2496	0.3081	0.2369	0.2467	0.3182
J_6	1.6461	1.6685	1.3634	1.1012	0.9890	0.5911	1.1735	1.0973	1.0175
J_7	0.2603	0.2656	0.2890	0.2336	0.2387	0.2368	0.2127	0.2232	0.2644
J_8	0.8381	0.8548	0.9572	0.8528	0.8788	0.9687	0.7866	0.8362	1.0196
J_9	0.2791	0.2904	0.2988	0.2040	0.2211	0.2060	0.2253	0.2422	0.2730
J_{10}	0.5054	0.5172	0.4821	0.5060	0.5103	0.4938	0.5954	0.6098	0.6052
J_{11}	2.56E-02	2.36E-02	3.16E-02	2.68E-02	2.49E-02	2.87E-02	2.64E-02	2.35E-02	3.23E-02
J_{12}	2.92E-03	2.95E-03	2.54E-03	1.96E-03	1.96E-03	1.96E-03	2.85E-03	2.70E-03	1.79E-03
J_{13}	1.0082	1.0220	0.8351	0.6745	0.6058	0.3621	0.7188	0.6721	0.6232

Table 2 Maximum evaluation criteria for Mexico earthquake

Criteria	Passive control			Semi-active control			Sample active control		
	Uniform	Multiple excitation, v_s		Uniform	Multiple excitation, v_s		Uniform	Multiple excitation, v_s	
	∞ m/s	3000 m/s	1000 m/s	∞ m/s	3000 m/s	1000 m/s	∞ m/s	3000 m/s	1000 m/s
J_1	0.4577	0.4036	0.3668	0.4197	0.4687	0.4565	0.3618	0.3451	0.3682
J_2	1.2930	1.1622	1.0222	1.2012	1.0637	1.0987	0.9010	0.8622	1.0192
J_3	0.6223	0.5564	0.3985	0.4156	0.3662	0.3204	0.4243	0.4068	0.3774
J_4	0.7974	0.7638	0.5719	0.6293	0.6582	0.6319	0.7466	0.7258	0.6718
J_5	0.1086	0.1191	0.1783	0.1429	0.1688	0.1759	0.1034	0.1153	0.1822
J_6	2.5067	2.3616	1.4720	1.0023	0.9963	0.9836	1.7894	1.8061	1.4952
J_7	0.3979	0.3919	0.3895	0.3501	0.3612	0.3146	0.2490	0.2633	0.3003
J_8	1.0014	1.0014	1.0301	1.0309	1.1397	1.1026	0.8236	0.8857	1.0417
J_9	0.4985	0.4923	0.4352	0.3047	0.3224	0.2642	0.2981	0.3126	0.3340
J_{10}	0.7560	0.7204	0.5273	0.5612	0.6045	0.5878	0.7509	0.7692	0.7605
J_{11}	1.65E-02	1.68E-02	2.20E-02	1.52E-02	1.61E-02	1.63E-02	1.38E-02	1.43E-02	1.81E-02
J_{12}	2.45E-03	2.35E-03	1.73E-03	1.96E-03	1.96E-03	1.96E-03	1.66E-03	1.52E-03	1.45E-03
J_{13}	1.3651	1.2860	0.8016	0.5458	0.5426	0.5357	0.9744	0.9835	0.8142

Table 3 Maximum evaluation criteria for Gebze earthquake

Criteria	Passive control			Semi-active control			Sample active control		
	Uniform	Multiple excitation, v_s		Uniform	Multiple excitation, v_s		Uniform	Multiple excitation, v_s	
	∞ m/s	3000 m/s	1000 m/s	∞ m/s	3000 m/s	1000 m/s	∞ m/s	3000 m/s	1000 m/s
J_1	0.4154	0.4273	0.4551	0.4988	0.5396	0.4646	0.4216	0.4384	0.4845
J_2	1.0608	1.0308	1.0294	1.1234	1.4687	1.1759	0.7441	0.9314	0.9434
J_3	0.4748	0.4377	0.4353	0.3552	0.4029	0.3646	0.3918	0.4196	0.4447
J_4	0.7562	0.8285	0.7809	0.6491	0.6550	0.7667	0.7965	0.8715	0.8602
J_5	0.2117	0.1887	0.2218	0.2208	0.2116	0.2256	0.1877	0.1822	0.2199
J_6	1.8458	1.8431	1.6656	1.7130	1.6967	1.4861	2.2908	2.2833	2.2086
J_7	0.4110	0.4080	0.3982	0.3270	0.3223	0.3167	0.2995	0.3037	0.3270
J_8	1.0453	1.0848	1.0841	0.9583	1.0925	1.0789	0.8577	0.9301	1.0061
J_9	0.4736	0.4718	0.4689	0.3386	0.3394	0.3481	0.3885	0.3956	0.4182
J_{10}	0.5416	0.5937	0.6913	0.6828	0.6929	0.7018	0.7000	0.7457	0.8551
J_{11}	1.88E-02	1.79E-02	2.18E-02	1.76E-02	1.65E-02	2.02E-02	1.67E-02	1.49E-02	2.08E-02
J_{12}	2.42E-03	2.42E-03	2.25E-03	1.96E-03	1.96E-03	1.96E-03	2.92E-03	2.71E-03	2.08E-03
J_{13}	0.8054	0.8043	0.7268	0.7475	0.7404	0.6485	0.9996	0.9963	0.9637

course at the expense of increasing deck displacement. The passive control system creates a larger force response reduction comparable to an active controlled system, while sacrificing deck displacement of the bridge structure. To reduce the excessive displacement, higher stiffness is needed between the deck and the towers and optimum performance with a passive control system can be obtained by balancing the reduction in forces along the bridge against tolerable displacements. For the CSB control, it is observed that unlike the passive control system case, the proposed active and semi-active control strategies are able to effectively and simultaneously reduce the maximum displacement and force responses. But the passive control system for this benchmark problem is a little better than the semi-active control strategy in some responses. Furthermore, multiple-support excitation can cause a significant increase in structural force responses; hence, it should be included in the analysis since it can excite entirely different modes than uniform-support excitation. Moreover, multiple-support excitation induces forces that are caused by pseudo-static displacements and can not be controlled. The force peak responses and normed responses over the entire record are significantly increased with the multiple excitation of low shear wave velocity, while the deck displacement response J_6 is decreased. Special attention needs to be given to the coupled modes since their control can lead to an increased force response of

the structure. The assumption of uniform motion along the entire bridge results in quantitative and qualitative differences in seismic response as compared with those produced by uniform motion at all supports.

The analyses performed shows that the spatial variation of the earthquake ground motion can significantly affect the structural response; consequently efficient control systems must be appropriately designed and tuned. Figure 5 shows the variation of maximum cable deviation, deck displacement and normed deck shear performance indices for different control strategies (Passive control (PC), Semi-active control (SAC) and Active control (AC)) under uniform and non-uniform excitations with different shear wave velocities. The time delay is caused by the apparent propagation velocity result in out-of phase motion at the bridge structure supports, which leads to a decrease of the deck displacement and an increase of the force response and cable deviation. From the statistical analysis of the variation of the evaluation criteria of different control strategies, the semi-active control has almost the same robustness stability of active control regarding the spatial variability of earthquake ground motions. Figure 6 shows the shear force response at Pier 2 for the El Centro earthquake ground motion with uniform and non-uniform ground motion with shear velocity 1000

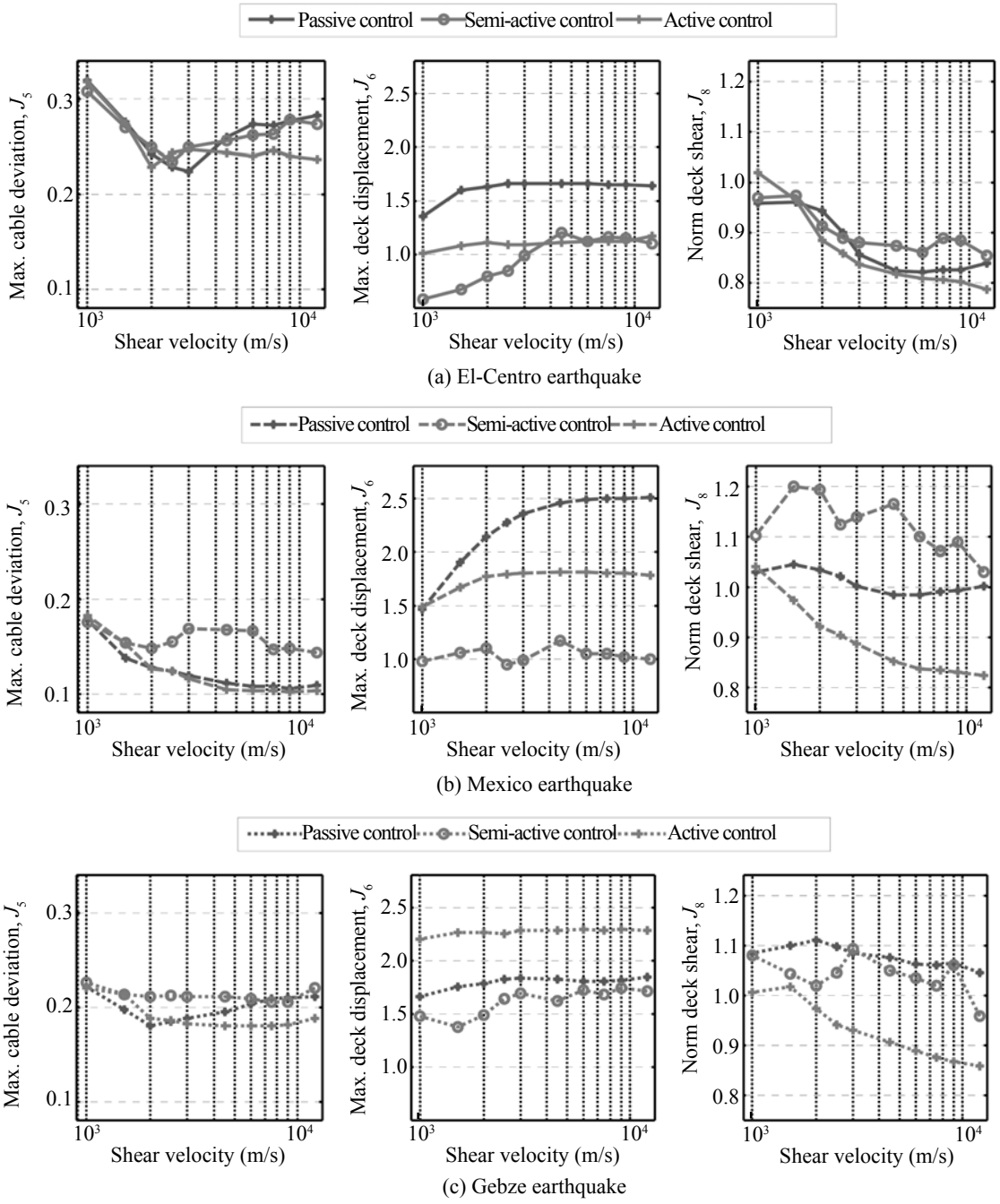

Fig. 5 Variation of different evaluation criteria with ground motion shear velocity

m/s for different control strategies. The spatial variation of ground motion affects the internal force demands, and consequently could affect the control efficiency. Nevertheless, in most engineering cases, this effect is still ignored by practical structural designers since seismic design codes remain unsatisfactory in terms of the ground motion spatial variations. This ignorance could reduce the degree of seismic safety and control system reliability of a CSB structure.

Figures 7 and 8 show the hysteretic loops of control devices for passive and semi-active control strategies under uniform and non-uniform excitations. It can be observed that the efficiency of the control devices is decreased, which can be attributed to excitation of primarily anti-symmetric higher modes by spatially variable input motions that are difficult to control. The control system should be designed not only to mitigate the dynamic component of the structural response, but also to counteract the effects of the pseudo-static component of the response.

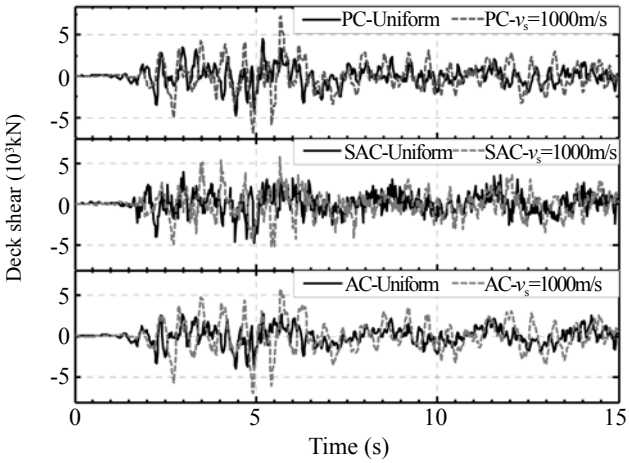

Fig. 6 Deck shear time history response to El Centro earthquake

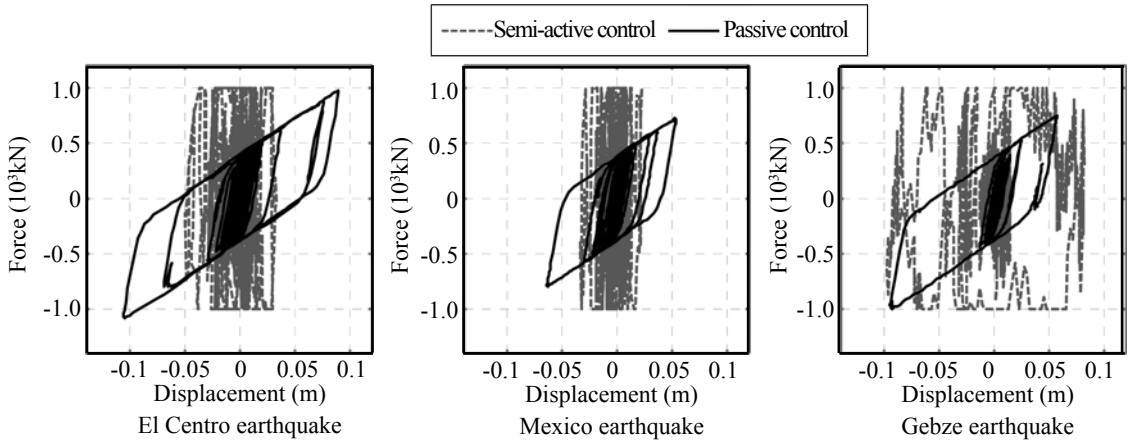

Fig. 7 Hysteresis loops of control devices under non-uniform excitation (v_s = 1000 m/s)

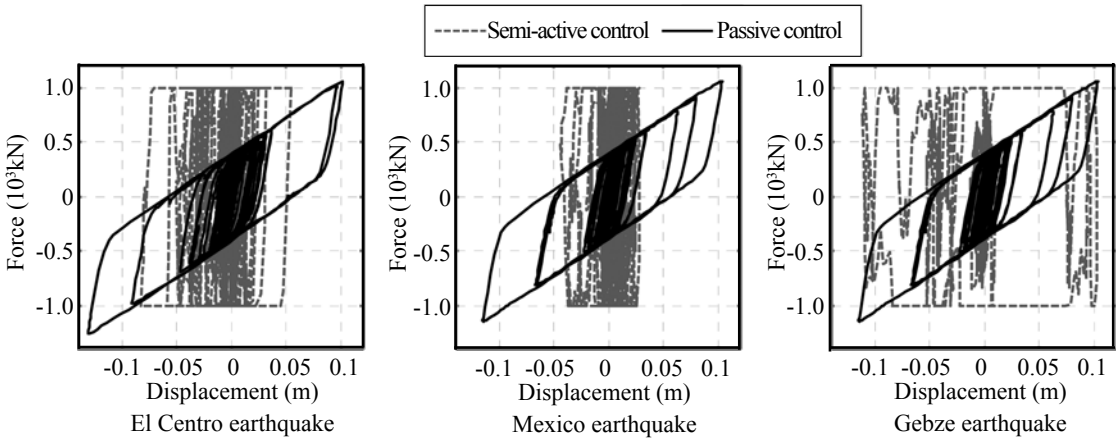

Fig. 8 Hysteresis loops of control devices under uniform excitation

5 Conclusions

This paper addresses the effect of spatial variations of ground motion with different wave propagation apparent velocities on the seismic performance of different control strategies of cable-stayed bridges (CSBs). The effectiveness of the proposed control strategies has been demonstrated and evaluated through application to the ASCE benchmark CSB problem subject to three historically recorded earthquakes. Three types of control

strategies were used to reduce the response of the deck, which includes actuators for active control, UHYDE-fbr friction for semi-active control and LRBs for passive control base isolations. The modified Bouc-Wen model was considered as a dynamic model for the control devices. Simulation results showed that significant reduction in earthquake induced forces along the bridge can be achieved with the different control strategies as compared to the case of using conventional connections. Moreover, the different proposed control systems can significantly reduce the seismic forces transferred to the towers of the bridge with an acceptable increase in deck displacement, and simultaneously keep tensions in the stay cables within a recommended range of allowable values with very small deviation from the nominal pretension. From the seismic response of the controlled bridge, it can be concluded that the efficiency of the control strategies depends significantly on the frequency content of the input motion. Unlike the passive control strategy, the proposed active and semi-active control strategies are able to effectively and simultaneously reduce the maximum displacement and force responses. It was observed that the different control strategies are quite effective in reducing the response quantities of the bridge whenever the predominant period of ground motions is close to the fundamental natural period of the bridge and significantly less effective in the contrary case.

The controlled systems perform well when earthquake motions are uniform at all supports along the entire CSB; however, under spatial variable excitations, the performance of the controlled systems with the considered parameters deteriorates over almost all of the evaluation criteria. Moreover, bridges subjected to spatially variable input motions are characterized by excitation of higher modes, which are primarily anti-symmetric and difficult to control, and hence reduce the efficiency of the control devices in energy dissipation. The assumption of uniform earthquake motion along the entire bridge could result in quantitative and qualitative differences in seismic response as compared with those produced by uniform motion at all supports. The semi-active control has almost the same robustness stability as the active control with regard to the spatial variability of the earthquake ground motions. Design codes and retrofitting techniques must be upgraded to take into account the spatial variation of the seismic input, and lack of consideration to the traveling wave effect may lead to unsafe conclusions.

Note that the above conclusions hold only for the bridge considered, and cannot be generalized to bridges of different types. The only general conclusion is that the effect of spatial variability of ground motion on the seismic response control of a bridge is a very complex problem, and depends on various parameters describing the structure and the characteristics of the seismic ground motion. The spatial variation of seismic ground motions plays a significant role in the safety of long span bridges and affects the efficiency of the structural control.

Acknowledgement

The authors gratefully acknowledge this research support of the Alexander von Humboldt Foundation (IV–AGY/1117497 STP) through the first author's postdoctoral fellowship award in Kassel University – Germany and the Japan Society for the Promotion of Science (P06138) through a postdoctoral fellowship award in Hokkaido University – Japan.

References

Abdel Raheem SE and Dorka UE (2006), "Feasibility Study on Semi-active Control of the Cable-stayed Bridge Benchmark with Friction Device System," *4th World Conference on Structural Control and Monitoring*, 4WCSCM, 11-13 July 2006, San Diego, California, Paper No. 32.

Abdel Raheem SE, Dorka UE and Hayashikawa T (2007), "Friction Based Semi-active Control of Cable-stayed Bridges," *JSCE Journal of Structural Engineering*, **53A**: 428–438.

Abdel Raheem SE and Hayashikawa T (2003), "Parametric Study on Steel Tower Seismic Response of Cable-stayed Bridges Under Great Earthquake Ground Motion," *JSCE Structural Engineering/Earthquake Engineering*, **20**(1): 25–41.

Abdel Raheem SE and Hayashikawa T (2007), "Seismic Protection of Cable-stayed Bridges Under Multiple-Support Excitations," *4th International Earthquake geotechnical Engineering*, Thessaloniki, Greece, 25–28 June 2007, Paper No. 1361.

Abdel Raheem SE, Hayashikawa T and Dorka U (2008), "Spatial Variation Effects on Seismic Response Control of Cable-stayed Bridges," *14th World Conference on Earthquake Engineering*, Beijing, China, 12-17 October 2008, Paper No. 05-02-0015.

Ali HM and Abdel-Ghaffar AM (1995a), "Modeling the Nonlinear Seismic Behavior of Cable-stayed Bridges with Passive Control Bearings," *Computers & Structures*, **54**(3): 461–492.

Ali HM and Abdel-Ghaffar AM (1995b), "Seismic Passive Control of Cable-stayed Bridges," *Shock and Vibration*, **2**(4): 259–272.

Caicedo JM, Dyke SJ, Moon SJ, Bergman LA, Turan G and Hague S (2003), "Phase II Benchmark Control Problem for Seismic Response of Cable-stayed Bridges," *Journal of Structural Control*, **10**: 137–168.

Dorka UE, Flygare E and Ji A (1998), "Passive Seismic Control of Bridges by Hysteretic Device System," *2nd World Conference on Structural Control*, Kyoto, Japan, June 27 –July 1, 1998: 1687–1694.

Dyke SJ, Spencer JR, Sain MK and Carlson JD (1996), "Modeling and Control of Magnetorheological Dampers for Seismic Response Reduction," *Smart Materials and Structures*, **5**: 565–575.

Dyke SJ, Turan G., Caicedo JM, Bergman LA and Hague S (2000), "Benchmark Control Problem for Seismic Response of Cable-stayed Bridges," http: //wusceel.civewustl.edu/quake.

Fujino Y (2002), "Vibration, Control and Monitoring of Long-span Bridges-recent Research, Developments and Practice in Japan," *Journal of Constructional Steel Research*, **58**: 71–97.

Ganev T, Yamazaki F, Ishizaki H and Kitazawa M (1998), "Response Analysis of the Higashi Kobe Bridge and Surrounding Soil in the 1995 Hyogoken Nanbu Earthquake," *Earthquake Engineering and Structural Dynamics*, **27**: 557–576.

Harichandran RS, Hawwari A and Sweidan BN (1996), "Response of Long-span Bridges to Spatially Varying Ground Motion," *Journal of Structural Engineering*, **122**: 476–484.

Iemura H and Pradono MH (2002), "Passive and Semi-active Seismic Response Control of a Cable-stayed Bridge," *Journal of Structural Control*, **9**: 189–204.

Jansen LM and Dyke SJ (2002), "Semi-active Control Strategies for MR Dampers: Comparative Study," *Journal of Engineering Mechanics*, **126**(8): 795–803.

Lin JH and Zhang YH (2005), *Vibration and Shock Handbook*, Chapter 30: "Seismic Random Vibration of Long-span Structures," CRC Press, Taylor & Francis: Boca Raton, FL 2005.

Lin JH, Zhang YH, Li QS and Williams FW (2004), "Seismic Spatial Effects for Long-span Bridges, Using the Pseudo Excitation Method," *Engineering Structures*, **26**:1207–1216.

Robinson WH (1982), "Lead-rubber Hysteretic Bearings Suitable for Protecting Structures During Earthquakes," *Earthquake Engineering and Structural Dynamics*, **10**: 593–604.

Saxena V, Deodatis G and Shinozuka M (2000), "Effect of Spatial Variation of Earthquake Ground Motion on the Nonlinear Dynamic Response of Highway Bridges," *12th World Conference on Earthquake Engineering*, Kyoto-Japan, Paper No. 2227.

Soong TT, *Active Structural Control, Theory and Practice*, Longman: UK, 1990.

Soyluk K and Dumanoglu AA (2004), "Spatial Variability Effects of Ground Motions on Cable-stayed Bridges," *Soil Dynamics and Earthquake Engineering*, **24**: 241–250.

Soyluk K, Domanoglu AA and Tuna ME (2004), "Random Vibration and Deterministic Analysis of Cable-stayed Bridges to Asynchronous Ground Motion," *Structural Engineering and Mechanics,* **18**(2).

Zerva A (1991), "Effect of Spatial Variability and Propagation of Seismic Ground Motions on the Response of Multiply Supported Structures," *Probability Engineering Mechanics*, **6**: 212–221.